

## Degeneracy at 1871 keV in $^{112}\text{Cd}$ and implications for neutrinoless double electron capture

K. L. Green,<sup>1,\*</sup> P. E. Garrett,<sup>1</sup> R. A. E. Austin,<sup>2</sup> G. C. Ball,<sup>3</sup> D. S. Bandyopadhyay,<sup>3</sup> S. Colosimo,<sup>2,†</sup> D. Cross,<sup>4</sup> G. A. Demand,<sup>1,‡</sup> G. F. Grinyer,<sup>1,§</sup> G. Hackman,<sup>3</sup> W. D. Kulp,<sup>5</sup> K. G. Leach,<sup>1</sup> A. C. Morton,<sup>3</sup> C. J. Pearson,<sup>3</sup> A. A. Phillips,<sup>1</sup> M. A. Schumaker,<sup>1,||</sup> C. E. Svensson,<sup>1</sup> J. Wong,<sup>1</sup> J. L. Wood,<sup>5</sup> and S. W. Yates<sup>6</sup>

<sup>1</sup>*Department of Physics, University of Guelph, Guelph, Ontario, N1G 2W1, Canada*

<sup>2</sup>*Department of Astronomy and Physics, Saint Mary's University, Halifax, Nova Scotia, B3H 3C3, Canada*

<sup>3</sup>*TRIUMF, 4004 Wesbrook Mall, Vancouver, British Columbia, V6T 2A3, Canada*

<sup>4</sup>*Department of Chemistry, Simon Fraser University, Burnaby, British Columbia, V5A 1S6, Canada*

<sup>5</sup>*School of Physics, Georgia Institute of Technology, Atlanta, Georgia 30332-0430, USA*

<sup>6</sup>*Departments of Chemistry and Physics & Astronomy, University of Kentucky, Lexington, Kentucky 40506-0055, USA*

(Received 22 July 2009; published 9 September 2009)

High-statistics  $\beta$ -decay measurements of  $^{112}\text{Ag}$  and  $^{112}\text{In}$  were performed to study the structure of the  $^{112}\text{Cd}$  nucleus. The precise energies of the doublet of levels at 1871 keV, for which the  $0^+$  member has been suggested as a possible daughter state following neutrinoless double electron capture of  $^{112}\text{Sn}$ , were determined to be 1871.137(72) keV ( $0_4^+$  level) and 1870.743(54) keV ( $4_2^+$  level). The nature of the  $0_4^+$  level, required for the calculation of the nuclear matrix element that would be needed to extract a neutrino mass from neutrinoless double electron capture to this state, is suggested to be of intruder origin.

DOI: 10.1103/PhysRevC.80.032502

PACS number(s): 23.20.Lv, 24.80.+y, 23.40.Bw

One of the most pressing issues in subatomic physics today is the question of the nature of the neutrino. The observation of neutrino oscillations [1–3] has revealed neutrino mixing and that neutrinos are massive particles or, more precisely, that at least two of the mass eigenstates are nonzero. However, it is still unknown if neutrinos are their own antiparticles (Majorana) or distinct from their antiparticles (Dirac). Furthermore, the oscillation experiments yield information on  $(\Delta m)^2$ , and thus the masses and their orderings remain unknown. Observation of neutrinoless double- $\beta$ -decay,  $\beta\beta(0\nu)$ , would reveal the Majorana nature of neutrinos, and a measure of the decay rate,  $\lambda^{0\nu}$ , would provide information on the neutrino masses via

$$\lambda^{0\nu} = \ln 2 G_{0\nu}(Q_{\beta\beta}, Z) |M_{0\nu}|^2 \langle m_{\beta\beta} \rangle^2. \quad (1)$$

The  $G_{0\nu}(Q_{\beta\beta}, Z)$  factor is the phase-space integral including the Fermi function,  $M_{0\nu}$  is the nuclear matrix element, and

$$\langle m_{\beta\beta} \rangle = \left| \sum_k m_k U_{ek}^2 \right| \quad (2)$$

is the effective Majorana neutrino mass in the  $\beta\beta(0\nu)$  process, with  $U_{ek}$  as the neutrino mixing matrix elements for the mass eigenstates  $m_k$ .

For  $\beta\beta(0\nu)$  searches, the typical signature is a peak at  $Q(\beta\beta)$  in the sum- $\beta$ -energy spectrum. However, such searches must strongly suppress the backgrounds from natural radioactivity and cosmic rays. A new class of  $\beta\beta(0\nu)$  experiments will attempt to surmount these problems; however, the neutrinoless double electron capture, ECEC( $0\nu$ ), process offers a potentially attractive alternative.

The basic physics of the ECEC process was outlined some time ago [4] and included an estimate of the radiative ECEC( $0\nu$ ) process, which was further refined in Ref. [5]. Following the formation of a virtual capture state with two electron holes in the  $1s$  shell, an internal bremsstrahlung (IB) photon is emitted accompanied by an electron transition from the  $2p$  to the  $1s$  shell. The IB photon is emitted at an energy  $E_{\text{IB}}$  of

$$E_{\text{IB}} = \Delta m - E(e_1) - E(e_2) - E_{\text{ex}}, \quad (3)$$

where  $\Delta m$  is the difference in the initial and final atomic masses,  $E_{\text{ex}}$  is the excitation energy in the daughter nucleus, and  $E(e_i)$  is the binding energy of the resulting electron hole in the final state. The normal IB process involves a transition of one of the electrons to an intermediate state from which it is captured, and this process dominates for large  $Q$  values. However, for small  $Q$  values, where both electrons may be captured leading to a virtual two-electron-hole atom, the process has a resonant enhancement when  $Q \equiv \Delta m - E(1S) - E(2P) - E_{\text{ex}} = Q_{\text{res}} \equiv E(2P) - E(1S)$ ; i.e., the radiative IB photon energy matches the  $K_\alpha$  hypersatellite x-ray energy [6]. In this case,

$$\lambda^{0\nu} \propto \frac{\Gamma^f(2P - 1S)}{(Q - Q_{\text{res}})^2 + \left(\frac{\Gamma^f}{2}\right)^2} |M_{0\nu}|^2 \langle m_{\beta\beta} \rangle^2, \quad (4)$$

and for favorable cases where  $Q = Q_{\text{res}}$ ,  $\lambda^{0\nu}$  may be enhanced by several orders of magnitude [6].

\*kgreen01@physics.uoguelph.ca

†Present address: Department of Physics, University of Liverpool, Liverpool, L69 7ZE, UK.

‡Department of Physics, Engineering Physics, and Astronomy, Queen's University, Kingston, Ontario, K7L 3N6, Canada.

§Present address: National Superconducting Cyclotron Laboratory, Michigan State University, East Lansing, Michigan 48824, USA.

||Present address: Department of Physics, Laurentian University, Sudbury, Ontario, P3E 2C6, Canada.

The condition  $Q \simeq Q_{\text{res}}$  is, in general, not satisfied by ground-state-to-ground-state decays. However, there are several cases in which an excited  $0^+$  state exists in the daughter nucleus that may approximately fulfill this condition. One of the most promising cases [5] exists for the  $^{112}\text{Sn} \rightarrow ^{112}\text{Cd}$  ECEC to the  $0_4^+$  level at 1871 keV. Using the 2003 atomic mass evaluation [7], a  $Q$  value of 1919.2(4.2) keV gives a difference of

$$Q - Q_{\text{res}} = -5.9(4.2) \text{ keV.} \quad (5)$$

Very recent mass measurements using the Penning trap at Jyväskylä give  $Q = 1919.82(16)$  keV, indicating that the  $^{112}\text{Sn} \rightarrow ^{112}\text{Cd}$  double EC to the  $0_4^+$  level may not undergo a resonant enhancement [8]. However, significant uncertainty remains because there exists a doublet of levels ( $0_4^+, 4_2^+$ ) at 1871 keV in  $^{112}\text{Cd}$ . Previously, the uncertainty on the 1871-keV,  $0_4^+$  level, for which there are no unique decaying transitions, has been quoted as 190 eV [9] or 130 eV [10]. However, as the level energies of this doublet were previously determined by  $\gamma$ -ray singles measurements, it is probable that the uncertainty has been considerably underestimated and may be as high as 1 keV. In the present work, an accurate determination of the  $0_4^+$  energy, obtained through coincidence  $\gamma$ -ray spectroscopy following  $^{112}\text{In}/^{112}\text{Ag}$   $\beta$  decay, is reported. Also reported is a new set of branching ratios (or limits) on the decay of the  $0_4^+$  level that reveals its nature as a member of the 2p-4h intruder configuration. The latter is an important consideration for subsequent calculation of the nuclear matrix element  $M_{0\nu}$ , which involves the overlap of the  $^{112}\text{Sn}$   $0^+$  ground state and the  $^{112}\text{Cd}$   $0_4^+$  level. This nuclear matrix element calculation would ultimately limit the determination of the  $\langle m_{\beta\beta} \rangle^2$  mass if the ECEC( $0\nu$ ) process were to be observed.

The experiment to investigate the structure of  $^{112}\text{Cd}$  was performed at the TRIUMF Isotope Separator and Accelerator (ISAC) facility in Vancouver, BC, Canada. The TRIUMF main cyclotron provided  $40\mu\text{A}$  of 500 MeV protons that were incident on a tantalum production target inducing spallation reactions. Among the reaction products were Ag and In, and these were extracted from the spallation target and ionized with the TRIUMF Resonant Ionization Laser Ion Source (TRILIS) [11]. The extracted ions passed through a mass separator, which selected  $A = 112$  products with a resultant cocktail beam of  $\sim 7.5 \times 10^6$  ions/s of  $^{112m}\text{In}$ ,  $\sim 2.3 \times 10^6$  ions/s of  $^{112}\text{In}$ , and  $\sim 4.8 \times 10^5$  ions/s of  $^{112}\text{Ag}$ . The beam was transported to the  $8\pi$   $\gamma$ -ray spectrometer [12], which consists of a spherically symmetric close-packed array of 20 Compton-suppressed HPGe detectors mounted around the beam-implantation site. The source to detector distance was  $\sim 14$  cm. The ions were deposited onto a continuous loop of aluminized Mylar tape in the center of the array. For the majority of the experiment, the beam was implanted onto the tape in 20-min cycles, with 20 min of implantation followed by 20 min of decay. This cycle was continued for 6 hours and was followed by a 6-hour-long decay. The data were collected for the duration of the run in scaled-down  $\gamma$  singles and  $\gamma\gamma$  coincidence mode, and  $\gamma\gamma$  matrices were constructed with a 150-ns coincidence time window. Approximately  $1 \times 10^8$  coincidence events

were sorted into a random-background-subtracted  $\gamma\gamma$  matrix. Immediately following the experiment, calibration data were collected using the decays from sealed  $^{152}\text{Eu}$ ,  $^{56}\text{Co}$ , and  $^{133}\text{Ba}$  sources.

The energies and intensities of the decaying  $\gamma$ -ray transitions were determined by fits to the  $\gamma$ -ray peaks present in the coincidence spectra. Peak centroids and areas were found employing the program GF3 [13]. The parameters describing the peak shape, specifically the  $\sigma$  of the Gaussian, height and decay constant of the exponential tail, as a function of peak position were determined by fitting the spectrum resulting from the application of a gate on the 617-keV  $2_1^+ \rightarrow 0_1^+$   $\gamma$  ray. The evolution of the peak shape parameters thus determined were held fixed for all coincidence spectra. The nonlinearity of the energy calibration was also calculated using the results from the fit of the 617-keV coincidence spectrum. The strong, well-resolved peaks were calibrated with precise energies determined previously [14]. It was found that an eighth-order polynomial was required to reproduce the data in detail, as shown in Fig. 1. The curve is expanded on the region from 100 keV to 2.0 MeV, which is the region of interest for the transitions from the 1871-keV  $4_2^+$  and  $0_4^+$  levels. Also shown for comparison in Fig. 1 is the fit resulting from a sixth-order polynomial which is insufficient to reproduce the nonlinear curve, especially in the critical 400-keV region. A standard deviation of 0.100 keV was calculated by comparing the  $\gamma$ -ray energies from the current experimental data to those previously determined, and was added in quadrature with the statistical uncertainties. The efficiency was determined by using RADWARE programs [13] to fit data from the calibration sources  $^{152}\text{Eu}$ ,  $^{56}\text{Co}$ , and  $^{133}\text{Ba}$ , with the intensities taken from *Table of Isotopes* [10]. A systematic 3% uncertainty on the relative efficiency curve was included that was added in quadrature to the statistical uncertainties of the  $\gamma$ -ray intensities. To determine the branching ratios, the coincidence spectrum was obtained by gating from above the level of

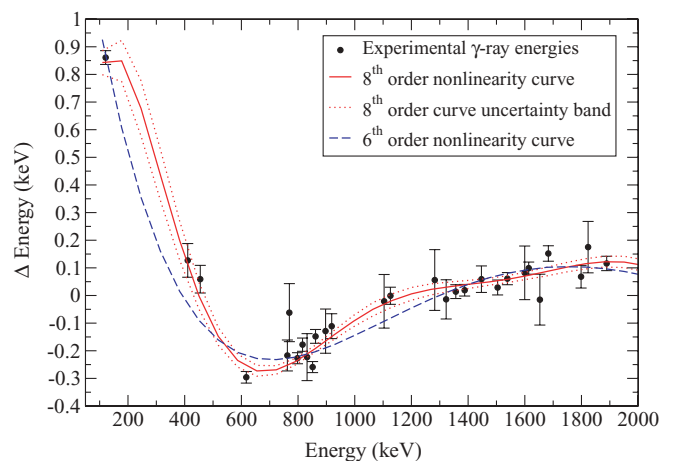


FIG. 1. (Color online) Fit of the nonlinearity of the energy calibration in the 100 keV to 2 MeV energy region. A total of 47  $\gamma$  rays with energies taken from Ref. [14] were used. The solid line is the eighth-order fit ( $\chi^2_{\nu} = 1.57$ ), with the dashed line outlining the  $1\sigma$  uncertainty band. The dotted line represents the sixth-order polynomial fit ( $\chi^2_{\nu} = 1.80$ ) to the nonlinearity curve.

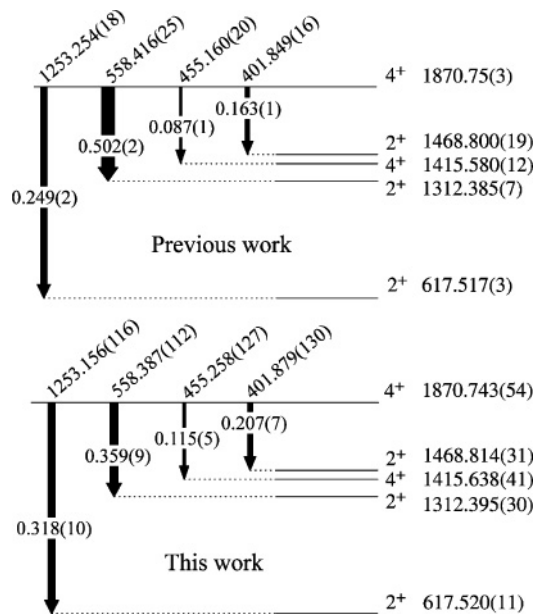


FIG. 2. Previous and current level schemes for decays from the 1871-keV  $4_2^+$  level. Transitions are labeled with  $\gamma$ -ray energies in keV. Previous energies are taken from Ref. [18], and branching ratios from Ref. [15]. Transition intensities sum to 1.000.

interest. The peak areas were converted into intensities and divided by the total intensity out of the specified level. Corrections due to summing effects were ignored because they have  $<1\%$  of an effect on the present branching ratios. Corrections from angular correlation effects were also ignored because the geometrical symmetry of the  $8\pi$  spectrometer generally results in less than a few percent effect on the  $\gamma$ -ray intensities. For the 1871-keV  $0_4^+$  level, angular correlations do not perturb the branching ratios, since the coincidence spectrum was obtained by gating on a feeding transition and all subsequent decaying  $\gamma$  rays are  $0^+ \rightarrow 2^+$  transitions.

The energies of the decaying transitions from the 1871-keV states were determined by fitting spectra created by gating on the transitions that uniquely feed each level. The partial level schemes highlighting the levels of interest, together with the previously assigned  $\gamma$ -ray decays, are shown in Figs. 2 and 3. The unique 1253-keV peaks from each level are shown in Fig. 4, where the centroids display a definite shift. A coincidence gate on the 996-keV  $\gamma$  ray, from the known 2867-keV  $3^-$  level [14], was used to identify the  $\gamma$  rays that depopulate the 1871-keV  $4^+$  level, i.e., the 402, 455, 558, and 1253-keV transitions. The coincidence spectrum for the 996-keV gate is shown in Fig. 5. The energies and branching ratios resulting from the fit are listed in Table I and in Fig. 2. The previous branching ratios were taken from Ref. [15], based on data tabulated in Ref. [16], where it was assumed that the  $(\alpha, 2n)$  reaction would not populate the  $0_4^+$  level. As can be seen, there is a very significant shift in the values, indicating that the above assumption was incorrect. The decay of the  $0_4^+$  level posed a greater challenge. In general, the population of states with spin  $\leq 2$  was much weaker than those of spin  $> 2$ , and thus identifying  $\gamma$  rays that uniquely feed the  $0_4^+$  level was far more difficult than for the  $4_2^+$  level. Ultimately, several transitions

TABLE I.  $\gamma$ -ray energies and branching ratios (BR) for the transitions from the  $0_4^+$  and  $4_2^+$  levels at 1871.137(72) and 1870.743(54) keV, respectively.

| $E_i$<br>(keV) | $E_\gamma^a$<br>(keV) | $E_f$<br>(keV) | BR <sup>b</sup> | Relative<br>$B(E2)$ |
|----------------|-----------------------|----------------|-----------------|---------------------|
| 1870.743(54)   | 1253.156(116)         | 617.520(11)    | 0.318(10)       | 0.5                 |
|                | 558.387(112)          | 1312.395(30)   | 0.359(9)        | 34                  |
|                | 455.258(127)          | 1415.638(41)   | 0.115(6)        | 26                  |
|                | 401.879(130)          | 1468.814(31)   | 0.207(9)        | 100                 |
| 1871.137(72)   | 1253.564(120)         | 617.520(11)    | 0.899(11)       | 3                   |
|                | 558.7 <sup>c</sup>    | 1312.395(30)   | $<0.05$         | $<9.7$              |
|                | 402.501(162)          | 1468.814(31)   | 0.101(11)       | 100                 |

<sup>a</sup>Uncertainty includes the 0.100 keV systematic uncertainty.

<sup>b</sup>Uncertainty on branching ratios does not take into account unobserved transitions.

<sup>c</sup>Transition unobserved in the present measurement. Branching ratio and relative  $B(E2)$  value are upper limits.

were identified, with the 958-keV coincidence spectrum shown in Fig. 6 being one of the strongest. Further, the 402-keV transition is far weaker compared to the 1253-keV  $\gamma$  ray than in the spectrum of Fig. 5. In addition, no evidence is found for a possible (and previously assigned [9]) 558-keV  $0_4^+ \rightarrow 2_2^+$  transition. Table I lists the results obtained for the  $0_4^+$  level, including the upper limit on the 558-keV branch using the procedure of Ref. [17]. The change in the branching ratios in Fig. 3 is again significant; where the previous values were obtained using thermal neutron  $(n, \gamma)$  data assuming the population of the  $4_2^+$  level was insignificant. However,  $^{113}\text{Cd}$  target impurities in the  $^{111}\text{Cd}$  target used in the  $(n, \gamma)$  study

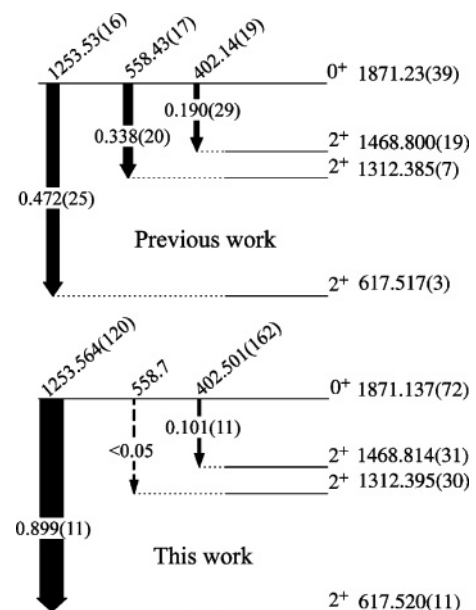


FIG. 3. Previous and current level schemes for decays from the 1871-keV  $0_4^+$  level. Transitions are labeled with  $\gamma$ -ray energies in keV. Previous energies are taken from Ref. [16], and branching ratios from Ref. [15]. Transition intensities sum to 1.000.

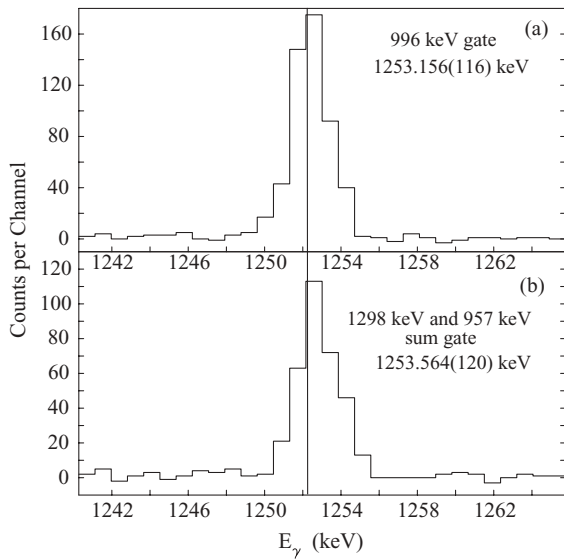


FIG. 4. Comparison between the 1253-keV peak centroids for the (a)  $\gamma$ -ray spectrum gated by the 996-keV transition feeding the 1871-keV  $4_2^+$  level and the (b)  $\gamma$ -ray sum spectrum gated by the 1298- and 958-keV transitions feeding the 1871-keV  $0_4^+$  level. The vertical line labels the centroid of the 1253-keV peak from the 996-keV gate.

could have given rise to a 558-keV peak (the  $^{114}\text{Cd}$ ,  $2_1^+ \rightarrow 0^+$  transition) not accounted for in Ref. [18].

The  $\gamma$ -ray energies determined here were used with the known 617.520(11) keV [14] level to determine the level energies through a least-squares fit method. The energy of the  $4_2^+$  level was thus determined to be 1870.743(54) keV, with the  $0_4^+$  level at an energy of 1871.137(72) keV. These energies are considered to be far more reliable than previous determinations due to the use of coincidence gating to isolate the transitions of interest from each of the doublet states. Using these more precise and accurate level energies, the difference in  $Q$  values is found to be  $Q - Q_{\text{res}} = -5.55(18)$  keV using the results of the new mass measurements [8].

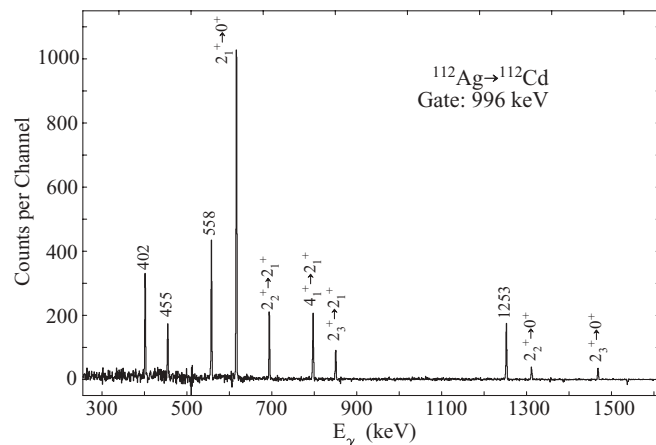


FIG. 5.  $\gamma$ -ray spectrum gated by the 996-keV transition feeding the 1871-keV  $4_2^+$  level. The energies of the  $\gamma$ -ray transitions from the  $4_2^+$  level are labeled in keV, with the remaining transitions labeled with their placements in the level scheme.

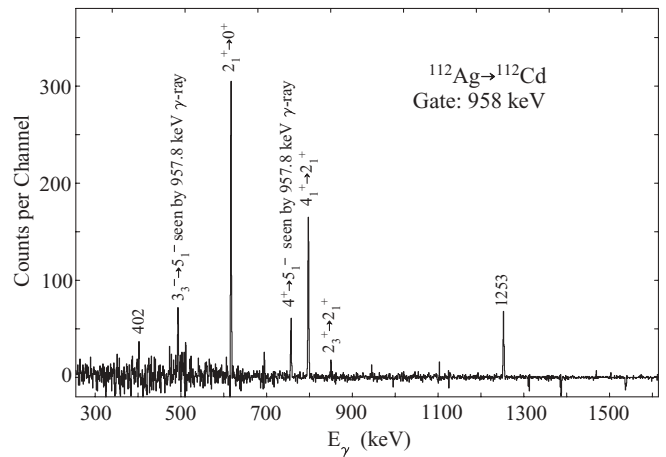


FIG. 6.  $\gamma$ -ray spectrum gated by the 958.0-keV transition feeding the 1871-keV  $0_4^+$  level. The energies of the  $\gamma$ -ray transitions from the  $0_4^+$  level are labeled in keV, with the remaining transitions labeled with their placements in the level scheme.

In the rate equation, Eq. (4), the nuclear matrix element would be an essential factor in the final determination of the neutrino mass from an observation of ECEC( $0\nu$ ) decay. The nature of the 1871-keV  $0_4^+$  state is necessary for the calculation of the nuclear matrix element that involves the overlap of the  $^{112}\text{Sn}$   $0^+$  ground state and the  $^{112}\text{Cd}$   $0_4^+$  level. The  $0_4^+$  level has typically been identified (see, e.g., Refs. [16,18–20]) as a member of the three-phonon vibrational quintuplet, being at approximately the correct energy and with a previously assigned [9] transition of 558 keV to the  $2_2^+$  two-phonon level. This assignment, however, was questioned in Ref. [15]. Further work [21], taking into account the systematics across the  $^{110}\text{Cd}$ – $^{116}\text{Cd}$  isotope chain, suggested that the  $0_4^+$  level has a dominant intruder character.

The systematics of low-lying  $0^+$  levels in the cadmium isotopes were shown in Fig. 6 of Ref. [21]. The  $0_4^+$  levels have excitation energies that display a v-shaped pattern as a function of the neutron number, which is characteristic of intruder state energy systematics. The reassignment of the  $0_4^+$  level from a member of the three-phonon quintuplet to an intruder state is further strengthened by the lack of any observed transition to the two-phonon states in the current work. The relative

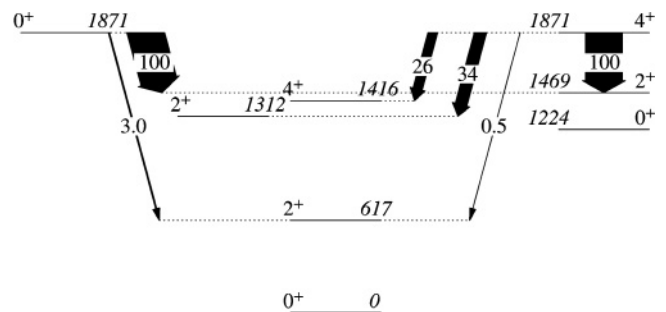


FIG. 7. Widths of the arrows give the relative  $B(E2)$  values for decays from the  $0_4^+$  and  $4_2^+$  1871-keV levels. Note the strong decay of the  $0_4^+$  state to the  $2^+$  intruder state at 1469 keV, which indicates that the  $0_4^+$  level has an intruder origin.



$B(E2)$  values presented in Fig. 7 indicate that the  $0_4^+$  state has the largest matrix element for decay to the  $2_3^+$  level at 1469 keV, which is assigned as a member of the intruder configuration.

In summary, the level structure of  $^{112}\text{Cd}$  has been investigated through high-statistics  $\beta$  decay of  $^{112}\text{In}$  and  $^{112}\text{Ag}$ . Using  $\gamma$ -ray coincidence spectroscopy, decays of the  $0^+$  and  $4^+$  doublet of levels at 1871 keV have been isolated, and precise level energies have been determined to be 1871.137(72) and 1870.743(54) keV, respectively. The precise level energy of the  $0_4^+$  state is necessary in calculating the  $Q$  value of the radiative neutrinoless double electron capture process, ECEC( $0\nu$ ), of the  $^{112}\text{Sn } 0^+$  ground state to the  $^{112}\text{Cd } 0_4^+$  1871-keV excited state. Using the recent mass measurement value [8], the  $Q - Q_{\text{res}}$  value is  $-5.55(18)$  keV, and it is concluded, in agreement with

Ref. [8], that the  $^{112}\text{Sn} \rightarrow ^{112}\text{Cd}$  ECEC( $0\nu$ ) process will not receive a substantial resonant enhancement. Further, the lack of evidence for the  $0_4^+$  to two-phonon  $2_2^+$  transition suggests that the  $0_4^+$  state is not a three-phonon state built on the ground state. From the observed decays and systematics of the  $0^+$  levels, it is concluded that the  $0_4^+$  state at 1871 keV is an excitation built on the 2p-4h intruder configuration, which would further complicate the calculation of the  $M_{0\nu}$  matrix element.

We would like to thank the TRILIS and ISAC groups who produced the  $^{112}\text{Ag}$  beam necessary for this work. This work was supported in part by the Natural Sciences and Engineering Research Council of Canada and the US DOE under Grant DE-FG02-96ER40958.

- 
- [1] M. F. Kidd, J. H. Esterline, and W. Tornow, *Phys. Rev. C* **78**, 035504 (2008).
- [2] J. Dawson, D. Degering, M. Köhler, R. Ramaswamy, C. Reeve, J. R. Wilson, and K. Zuber, *Phys. Rev. C* **78**, 035503 (2008).
- [3] A. S. Barabash, Ph. Hubert, A. Nachab, S. I. Konovalov, I. A. Vanyushin, and V. Umatov, *Nucl. Phys.* **A807**, 269 (2008).
- [4] R. G. Winter, *Phys. Rev.* **100**, 142 (1955).
- [5] J. Bernabeu, A. De Rujula, and C. Jarlskog, *Nucl. Phys.* **B223**, 15 (1983).
- [6] Z. Sujkowski and S. Wycech, *Phys. Rev. C* **70**, 052501(R) (2004).
- [7] G. Audi and A. Wapstra, *Nucl. Phys.* **A729**, 337 (2003).
- [8] S. Rahaman, V.-V. Elomaa, T. Eronen, J. Hakala, A. Jokinen, A. Kankainen, J. Rissanen, J. Suhonen, C. Weber, and J. Äystö, *Phys. Rev. Lett.* **103**, 042501 (2009).
- [9] D. de Frenne and E. Jacobs, *Nucl. Data Sheets* **79**, 639 (1996).
- [10] *Table of Isotopes*, 8th ed., edited by R. Firestone and V. Shirley (Wiley, New York, 1996).
- [11] C. Geppart, P. Bricault, R. Horn, J. Lassen, C. Rauth, and K. Wendt, *Nucl. Phys.* **A746**, 631c (2004).
- [12] C. E. Svensson, R. A. E. Austin, G. C. Ball, P. Finlay, G. F. Grinyer, G. S. Hackman, C. J. Osborne, F. Sarazi, H. C. Scraggs, M. B. Smith, and J. C. Waddington, *Nucl. Instrum. Methods Phys. Res. B* **204**, 660 (2003).
- [13] D. C. Radford, RADWARE Software Package, Oak Ridge National Laboratory, available at radware.phy.ornl.gov.
- [14] P. E. Garrett, H. Lehmann, J. Jolie, C. A. McGrath, M. Yeh, W. Younes, and S. W. Yates, *Phys. Rev. C* **64**, 024316 (2001).
- [15] P. E. Garrett, K. L. Green, H. Lehmann, J. Jolie, C. A. McGrath, M. Yeh, and S. W. Yates, *Phys. Rev. C* **75**, 054310 (2007).
- [16] M. Délèze, S. Drissi, J. Jolie, J. Kern, and J.-P. Vorlet, *Nucl. Phys.* **A554**, 1 (1993).
- [17] L. A. Currie, *Anal. Chem.* **40**, 586 (1968).
- [18] S. Drissi, P. A. Tercier, H. G. Börner, M. Délèze, F. Hoyler, S. Judge, J. Kern, S. J. Mannanal, G. Mouze, K. Schreckenbach, J.-P. Vorlet, N. Warr, A. Williams, and C. Ythier, *Nucl. Phys.* **A614**, 137 (1997).
- [19] J. Kern, P. E. Garrett, J. Jolie, and H. Lehmann, *Nucl. Phys.* **A593**, 21 (1995).
- [20] H. Lehmann, P. E. Garrett, J. Jolie, C. A. McGrath, M. Yeh, and S. W. Yates, *Phys. Lett.* **B387**, 259 (1996).
- [21] P. E. Garrett, K. L. Green, and J. L. Wood, *Phys. Rev. C* **78**, 044307 (2008).